# Support information

## The formation of uniform graphene-polyaniline hybrids using a completely miscible cosolvent that have an excellent electrochemical performance

Mei-li LIU†, Xiang LONG†, Hai-yan TANG, Xin-hang FAN, Chao-yi CHEN, Jiao-jing SHAO*

School of Materials and Metallurgy, Guizhou University, Guiyang 550025, China

E-mail: shaojiao_jing@163.com; xjshao@tju.edu.cn

†These authors contributed to this work equally.

## 1 Calculation of capacitances, power/energy densities.

The gravimetric, areal, and volumetric specific capacitances ($C$) were calculated based on the GCD profiles according to the following equations, respectively:

$$C_m(F \cdot g^{-1}) = \frac{2 \cdot I \cdot t}{m \cdot \Delta E} \quad (1)$$

$$C_S(F \cdot cm^{-2}) = \frac{2 \cdot I \cdot t}{S \cdot \Delta E} \quad (2)$$

$$C_V(F \cdot cm^{-3}) = \frac{2 \cdot I \cdot t}{V \cdot \Delta E} \quad (3)$$

Where $I$ represent current density, $t$ is discharge time, $\Delta E$ is potential window. $m$, $S$, $V$ represent the mass, surface area, and volume of a single fiber electrode, respectively.

The volumetric energy density ($E_V$) and power density ($P_V$) of the fiber supercapacitor are calculated based on the following equations, respectively:

$$E_V(mWh \cdot cm^{-3}) = \frac{C_V \cdot (\Delta E)^2}{2 \cdot 3.6} \quad (4)$$

$$P_V(mW \cdot cm^{-3}) = \frac{3600 \cdot E_V}{\Delta t} \quad (5)$$

## 2 Calculation of graphene and PANI loadings

In a typical fabrication of the graphene/PANI composite fiber, GO solid and PANI are mixed in the cosolvent to get a homogeneous gel dope for the following wet-spinning, chemical reduction treatment, and air-drying. Supposing the weight of GO solid and PANI are $M_1$ and $M_2$, respectively. After chemical reduction, the weight of the reduced GO is $M_3$ that is less than $M_1$ owing to the removal of oxygen-containing groups, while the weight of PANI keeps constant after reduction. Therefore, the weight percentages of graphene ($W_1$) and PANI ($W_2$) in the final composite fiber can be calculated according to $W_1=M_3/(M_2+M_3)$ and $W_2=M_2/(M_2+M_3)$, respectively. It should be noticed that $M_1$ and $M_2$ can be weighed, but $M_3$ cannot be weighed directly.

To get $M_3$, we need to know the weight percentage of the removed oxygen-containing groups during the chemical reduction of the GO precursor. Hence, pure GO solid of $m_1$ is reduced under the same chemical reduction treatment followed by air-drying, and the as-obtained reduced GO is weighed and supposing its weight is $m_3$, and consequently, the weight percentages of the removed oxygen-containing groups and the remaining reduced GO can be readily calculated according to $(m_1-m_3)/m_1$ and $m_3/m_1$, respectively. Next, the $M_3$ can be calculated based on the following formula $M_3=M_1 \times (m_3/m_1)$, and then, the $W_1$ and $W_2$ can be calculated. Finally, the graphene and PANI loading data are provided in the Table S1.

## 3 Figures and tables

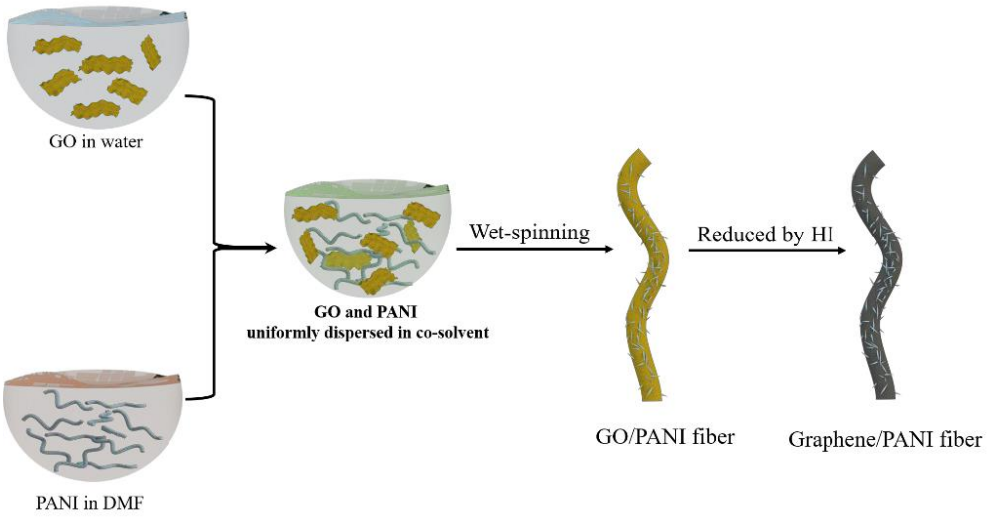


**Figure S1.** Schematic illustration of the preparation of the graphene/PANI composite fiber.

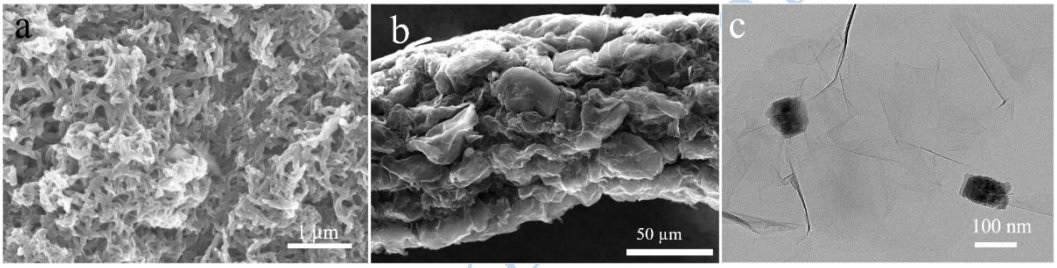


**Figure S2.** (a) SEM image of the PANI nanofibers synthesized by the fast polymerization method. (b) SEM and (c) TEM images of the GN/PANI-$H_2O$.

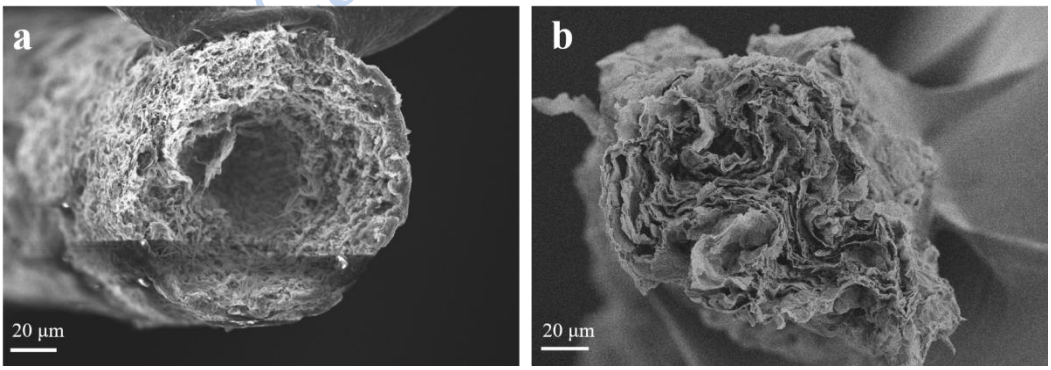


**Figure S3. (a)** the cross-section SEM image of GN/PANI-CS and (b) the cross-section SEM image of GN/PANI-$H_2O$.

$N_2$ adsorption-desorption measurement is conducted to investigate the pore structure of the fibers. As shown in the Figure S4a, the as-obtained isotherms are comparable and both are not closed, and the data points are very sparse in the isotherms and in the pore size distribution curves (Figure S4b). It is observed that the process of obtaining data points is very slow for both fiber samples during the $N_2$ adsorption-desorption measurement. The results and phenomena are possibly due to the compact microstructure and the rather low porosity of the composite fibers, which is also in agreement with the relatively long time constant (τ) as shown in the Bode plots (Figure 4e).

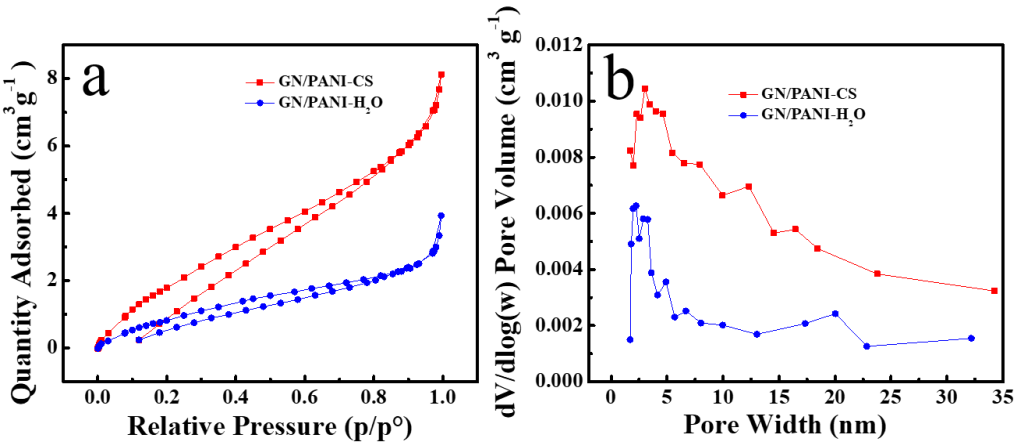


**Figure S4.** $N_2$ adsorption-desorption isotherms of the GN/PANI-CS (a) and GN/PANI-$H_2O$ (b) fibers.

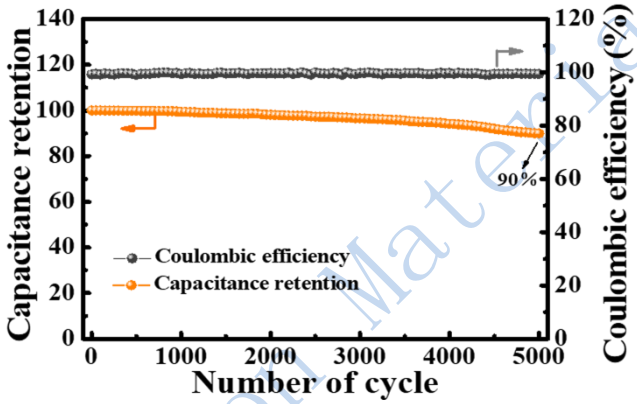


**Figure S5.** Cyclic performance at 1 A $g^{-1}$ of GN/PANI-CS.



**Table S1.** Electrochemical properties of GN/PANI-CS fibers with different ratio of PANI and GO precursors.

| Composite Fiber | Volumetric capacitance (F $cm^{-3}$) | Gravimetric capacitance (F $g^{-1}$) | Capacitance retention (%) (GCD) | Mass Loading (g $cm^{-3}$) | GO($W_1$) Content (%) | PANI($W_2$) Content (%) |
|---|---|---|---|---|---|---|
| Graphene/PANI-CS-20 | 244.2 | 119.75 | 47.7 | 2.04 | 92.5 | 7.5 |
| Graphene/PANI-CS-50 | 330.6 | 265.7 | 47.43 | 1.24 | 96.9 | 3.1 |
| Graphene/PANI-CS-70 | 179.3 | 73.9 | 35.2 | 2.43 | 97.7 | 2.3 |
| Graphene/PANI-CS-100 | 77.8 | 32.5 | 29.6 | 2.39 | 99.73 | 0.27 |

**Table S2.** Electrochemical performance of fiber supercapacitors with GN/PANI composite fiber electrodes

Advanced Materials, 2018, 30(18): 1800124.

| Electrodes | Electrolyte | Volumetric specific capacitance | Cycling Stability | Energy/power density | Journal & Publication Year | Mass Loading |
|---|---|---|---|---|---|---|
| GF-PANI | PVA/$H_3PO_4$ | 76.1 F $cm^{-3}$ at 0.1 mA $cm^{-2}$ | — | — | RSC Adv.[1] 2013 | — |
| (Graphene/CNTs) @PANI | PVA/$H_2SO_4$ | 36.7 F $cm^{-3}$ at 0.2 A $cm^{-3}$ | 80.6% after 2000 cycles at 0.1 V $s^{-1}$ | 0.98 mWh $cm^{-3}$ 16.25 mW $cm^{-3}$ | J. Colloid Interface. Sci.[2] 2017 | 6.44 g $cm^{-3}$ |
| PANI/RGO | PVA/$H_2SO_4$ | 148 F $cm^{-3}$ at 0.08 A $g^{-1}$ | 86.0% after 17 000 cycles at 1.26 A $g^{-1}$ | 8.80 mWh $cm^{-3}$ 30.77 mW $cm^{-3}$ | Adv. Mater.[3] 2018 | 1.39 g $cm^{-3}$ |
| GF@PANI | PVA/$H_2SO_4$ | 226.3 F $cm^{-3}$ at 2 mA $cm^{-2}$ | 96.8% after 5000 cycles | 5.70 mWh $cm^{-3}$ 167.7 mW $cm^{-3}$ | ACS Appl. Energy Mater[4] 2019 | — |
| PANI/GF | PVA/$H_3PO_4$ | 51.3 F $cm^{-3}$ at 0.22 mA $cm^{-2}$ | 100% after 10000 cycles at 0.22 mA $cm^{-2}$ | 226.4 mWh $cm^{-2}$ 12.2 μW h $cm^{-2}$ | Synth Met[5] 2020 | — |
| PANI @rEGO/GP | PVA/$H_3PO_4$ | 164.5 F $cm^{-3}$ at 0.25 A $cm^{-3}$ | 80.5% after 2000 cycles at 0.208 mA $cm^{-1}$ | 7.3 mWh $cm^{-3}$ 225.8 mW $cm^{-3}$ | Appl.Mater. Today[6] 2020 | — |
| GN/PANI-CS | PVA/$H_2SO_4$ | 330.6 F $cm^{-3}$ at 0.1A $g^{-1}$ | 85.0% after 20000 cycles at 1 A $cm^{-2}$ | 29.4 mWh $cm^{-3}$ 199 mW $cm^{-3}$ | This work | 1.24 g $cm^{-3}$ |
| GN/PANI-$H_2O$ | PVA/$H_2SO_4$ | 100.8 F $cm^{-3}$ at 0.1A $g^{-1}$ | — | 8.96 mWh $cm^{-3}$ 146.6 mW $cm^{-3}$ | This work | 3.32 g $cm^{-3}$ |

## References


[1] Huang T, Zheng B, Kou L, et al. Flexible high performance wet-spun graphene fiber supercapacitors [J]. RSC Advances, 2013, 3(46): 23957-23962.

[2] Liu D, Du P, Wei W, et al. Skeleton/skin structured (RGO/CNTs)@PANI composite fiber electrodes with excellent mechanical and electrochemical performance for all-solid-state symmetric supercapacitors [J]. J Colloid Interface Sci, 2018, 513: 295-303.

[3] Li P, Jin Z, Peng L, et al. Stretchable all-gel-state fiber-shaped supercapacitors enabled by macromolecularly interconnected 3D graphene/nanostructured conductive polymer hydrogels [J].

[4] Zheng X, Yao L, Qiu Y, et al. Core–sheath porous polyaniline nanorods/graphene fiber-shaped supercapacitors with high specific capacitance and rate capability [J]. ACS Applied Energy Materials, 2019, 2(6): 4335-4344.

[5] Zhang M, Wang X, Yang T, et al. Polyaniline/graphene hybrid fibers as electrodes for flexible supercapacitors [J]. Synthetic Metals, 2020, 268: 116484.

[6] Niu J, Li J, Liu P. Facile fabrication of flexible, bendable and knittable electrode with PANI in the well-defined porous rEGO/GP fiber for solid state supercapacitors [J]. Applied Materials Today, 2020, 20: 100733.